ARTICLE
Journal of Cellular Biochemistry 106:521–528 (2009)

Journal of Cellular Biochemistry

Dimerization of DNA Methyltransferase 1 Is Mediated by Its Regulatory Domain

Karin Fellinger,[1] Ulrich Rothbauer,[1] Max Felle,[2] Gernot Längst,[2] and Heinrich Leonhardt[1*]

[1]*Center for Integrated Protein Science at the Department of Biology II, Ludwig Maximilians University Munich, 82152 Planegg-Martinsried, Germany*

[2]*Institute for Biochemistry, Genetics and Microbiology, University of Regensburg, 93053 Regensburg, Germany*

ABSTRACT

DNA methylation is a major epigenetic modification and plays a crucial role in the regulation of gene expression. Within the family of DNA methyltransferases (Dnmts), Dnmt3a and 3b establish methylation marks during early development, while Dnmt1 maintains methylation patterns after DNA replication. The maintenance function of Dnmt1 is regulated by its large regulatory N-terminal domain that interacts with other chromatin factors and is essential for the recognition of hemi-methylated DNA. Gelfiltration analysis showed that purified Dnmt1 elutes at an apparent molecular weight corresponding to the size of a dimer. With protein interaction assays we could show that Dnmt1 interacts with itself through its N-terminal regulatory domain. By deletion analysis and co-immunoprecipitations we mapped the dimerization domain to the targeting sequence TS that is located in the center of the N-terminal domain (amino acids 310–629) and was previously shown to mediate replication independent association with heterochromatin at chromocenters. Further mutational analyses suggested that the dimeric complex has a bipartite interaction interface and is formed in a head-to-head orientation. Dnmt1 dimer formation could facilitate the discrimination of hemi-methylated target sites as has been found for other palindromic DNA sequence recognizing enzymes. These results assign an additional function to the TS domain and raise the interesting question how these functions are spatially and temporarily co-ordinated. J. Cell. Biochem. 106: 521–528, 2009.

KEY WORDS: DIMER; METHYLATION; DNA METHYLTRANSFERASE1; Dnmt1; TARGETING SEQUENCE

DNA methylation at cytosine residues of CpG dinucleotides is a crucial epigenetic modification that regulates gene expression and chromatin structure and is required for X chromosome inactivation and imprinting [Leonhardt and Cardoso, 2000; Bird, 2002]. In early development new methylation patterns are established by de novo methyltransferases Dnmt3a and 3b and are subsequently maintained by DNA methyltransferase1 (Dnmt1) [Hermann et al., 2004; Goll and Bestor, 2005]. Dnmt1 is the only methyltransferase with a preference for hemi-methylated DNA [Bestor and Ingram, 1983; Pradhan et al., 1999] generated by DNA replication and repair. Targeted disruption of the *dnmt1* gene leads to genome-wide loss of DNA methylation and embryonic lethality [Li et al., 1992]. Artificial reduction of cellular Dnmt1 levels severely affects development and genome stability [Gaudet et al., 2003, 2004]. The crucial role of Dnmt1 was recently also shown in human cells [Easwaran et al., 2004; Egger et al., 2006; Spada et al., 2007]. During S-phase Dnmt1 associates with the replication machinery by interacting with PCNA [Leonhardt et al., 1992; Chuang et al., 1997]. PCNA also targets Dnmt1 to DNA repair sites to restore the epigenetic information [Mortusewicz et al., 2005]. The interaction of Dnmt1 with the replication machinery enhances methylation efficiency by twofold, but is not strictly required for postreplicative maintenance of DNA methylation [Schermelleh et al., 2007; Spada et al., 2007]. The targeting sequence (TS domain) recruits Dnmt1 to pericentric heterochromatin independent of DNA replication, H3K9 trimethylation and the interacting proteins SUV39H1 and HP1 [Easwaran et al., 2004]. Both, the PCNA binding domain PBD and the heterochromatin binding TS domain, reside in the large N-terminal part of Dnmt1, a region of the protein that contains several regulatory functions and is unique among the family of DNA methyltransferases. The intramolecular interaction between the regulatory N-terminus and the catalytic C-terminus is essential for the catalytic activity of Dnmt1. Despite the presence of all typical, conserved methyltransferase motifs, the catalytic domain per se

Additional Supporting Information may be found in the online version of this article.

Grant sponsor: Deutsche Forschungsgemeinschaft (DFG); Grant sponsor: Nanosystems Initiative Munich (NIM).

*Correspondence to: Dr. Heinrich Leonhardt, Department of Biology II, Ludwig Maximilians University Munich, 82152 Planegg-Martinsried, Germany. E-mail: h.leonhardt@lmu.de

Received 18 December 2008; Accepted 22 December 2008 • DOI 10.1002/jcb.22071 • 2009 Wiley-Liss, Inc.
Published online 27 January 2009 in Wiley InterScience (www.interscience.wiley.com).

lacks methyltransferase activity [Zimmermann et al., 1997; Margot et al., 2000, 2003; Fatemi et al., 2001]. Also, interaction of Dnmt1 with the chromatin factors Np95, LSH, EZH2 and G9a was shown to be essential for maintenance of DNA methylation [Esteve et al., 2006; Vire et al., 2006; Bostick et al., 2007; Sharif et al., 2007; Myant and Stancheva, 2008]. The molecular mechanism of these multiple interactions controlling the activity of Dnmt1 and the recognition of hemi-methylated target sites remains largely unknown.

Our biochemical characterization shows that Dnmt1 forms a stable dimer. With gelfiltration, co-immunoprecipitation and in vivo assays we demonstrate that Dnmt1 dimerization is mediated by the N-terminal TS domain. These results show that the TS domain is not only crucial for recruitment of Dnmt1 to heterochromatin as reported previously, but also for the assembly of stable dimeric Dnmt1 complexes.

MATERIALS AND METHODS

EXPRESSION CONSTRUCTS

The expression construct for GFP-Dnmt1 was described previously [Easwaran et al., 2004]. GFP-Dnmt1 fusion constructs were generated by PCR cloning using eGFP-Dnmt1 as template to clone into pEGFP-N1 (Clontech) employing either the restriction sites *Xho*I and *Xma*I or *Bsr*GI and *Hin*dIII. GFP was subsequently replaced with mCherry [kindly provided by R.Y. Tsien, Shaner et al., 2004]. Throughout this study we used the enhanced GFP and monomeric Cherry. PCR primers are listed in Supplementary Table I. All constructs were sequenced and tested by transient expression in human embryonic kidney (HEK) 293T cells followed by immunoblot analysis. hTS was cloned into pMAL-2cX (NEB) after replacement of factor Xa cleavage site through a TEV cleavage site.

CELL CULTURE AND TRANSFECTION AND MICROSCOPY

HEK 293T HeLa and BHK cells were cultured in DMEM supplemented with 10% fetal calf serum and 50 μg/ml gentamycine. BHK cells carrying a *lac* operator array were maintained in the presence of 150 μg/ml hygromycin B (PAA Laboratories) [Tsukamoto et al., 2000]. HEK 293T cells were transfected with polyethyleneimine (Sigma). For microscopy, BHK cells were grown to 50–70% confluence on glass coverslips and co-transfected with TS-LacI-RFP and GFP-Dnmt1 constructs using Transfectin (Bio-Rad) according to manufacturer's instructions. Cells were fixed 24 h after transfection with 3.7% formaldehyde in PBS for 10 min at room temperature. After permeabilization with 0.2% Triton X-100 in PBS for 3 min cells were counterstaind with DAPI and mounted in Vectashield (Vector Laboratories). Microscopy was performed as described [Zolghadr et al., 2008].

CO-IMMUNOPRECIPITATION AND IMMUNOBLOTTING AND QUANTIFICATION

HEK 293T cells were transiently transfected with expression plasmids as described above. After 24 h, 60–90% of the cells expressed the constructs as determined by fluorescence microscopy. About $\sim 1 \times 10^7$ cells were harvested in 200 μl of lysis buffer (20 mM Tris/HCl pH 7.5, 150 mM or 1 M NaCl, 0.5 mM EDTA, 2 mM PMSF, 0.5% NP40). After clearing by centrifugation (10 min, 20,000*g*, 4°C) supernatants were adjusted to a volume of 500 μl with dilution buffer (lysis buffer without NP40). 50 μl aliquots were prepared in SDS-containing sample buffer (referred to as input (I)). Extracts were incubated with GFP Nanotrap [Rothbauer et al., 2008] (Chromotek) for 2 h at 4°C with constant mixing. Immunocomplexes were harvested by centrifugation (2 min, 5,000*g*, 4°C) and beads were washed twice with 1 ml of dilution buffer containing 300 mM NaCl and resuspended in SDS–PAGE sample buffer (referred to a bound (B)). Proteins were eluted by boiling at 95°C. For immunoblot analysis 1% of the input and 20% of the bound fractions were separated by SDS–PAGE and blotted onto a PVDF-membrane (Millipore). Antigens were detected with a mouse monoclonal anti-GFP antibody (Roche), a rat monoclonal anti-mCherry antibody [Rottach et al., 2008] or a rat monoclonal anti-DNMT1 antibody [Spada et al., 2007]. For quantification mean grey values of band intensities of co-precipitated proteins obtained from Western blots were calculated with the ImageJ software (Version 1.38, http://rsb.info.nih.gov/ij/). The ratios of bound and input signals were determined and the mean value and standard error from three independent experiments were calculated.

GELFILTRATION

Reference gelfiltration was carried out with a Superose 6 column and separation properties were determined in a first run with mass standard proteins (thyroglobulin (669 kDa), apoferritin (443 kDa), BSA (66 kDa)). For analysis of endogenous Dnmt1, HeLa cells were lysed in 200 μl of buffer (20 mM Tris/HCl pH 7.5, 50 mM NaCl, 0.5 mM EDTA, 2 mM PMSF, 0.5 mM NP40, 1 μg/μl DNase I, 5 mM $MgCl_2$), incubated on ice for 30 min and centrifuged (15 min, 20,000*g*, 4°C). The supernatant was adjusted to 500 μl with PBS and applied to a Superose 6 gelfiltration column (GE Healthcare) (Fig. 1). Recombinant human Dnmt1 and TS proteins were analyzed by a Superdex 200 column (GE Healthcare) (Fig. 3) in buffer containing 20 mM Tris, pH 7.5, 150 mM NaCl, 1 mM EDTA, 1 mM DTT. Chromatography was performed with a flow rate of 0.5 ml/min and fractions were analyzed by SDS–PAGE and immunoblotting with an antibody against human DNMT1.

PROTEIN PURIFICATION

DNMT1 containing an N-terminal His tag was purified from baculovirus infected Sf21 insect cells and purified by Ni-NTA chromatography as described previously [Yokochi and Robertson, 2002]. The DNMT1 virus was kindly provided by K.D. Robertson. DNMT1 was further purified on a Resource Q column (GE Healthcare) with a linear gradient from 100–600 mM NaCl in 20 mM Hepes, pH 7.9; 1 mM EDTA; 1.5 mM $MgCl_2$; 10% Glycerol; 1 mM DTT, 1 mM PMSF. The peak fractions were combined and stored at −80°C. The DNMT1 TS domain (pMAL-TS) was expressed in *E. coli* K12 TB1 cells (NEB) according to the manufacturer's instructions. Protein expression was induced at an OD_{600} of 0.7 with 0.3 mM IPTG for 2 h, cells were harvested and washed once with TBS. The cell pellet of 1 L culture was resuspended in 30 ml of buffer CV (20 mM Tris pH 7.5, 200 mM NaCl, 1 mM EDTA, 1 mM PMSF, 1 mM DTT) and cells were lysed (Branson Sonifier). The lysate was cleared (20,000*g*, 4°C, 20 min) and incubated with 10 ml amylose resin (NEB). The resin was washed 3× with 50 ml buffer CV and applied to a glass column. The

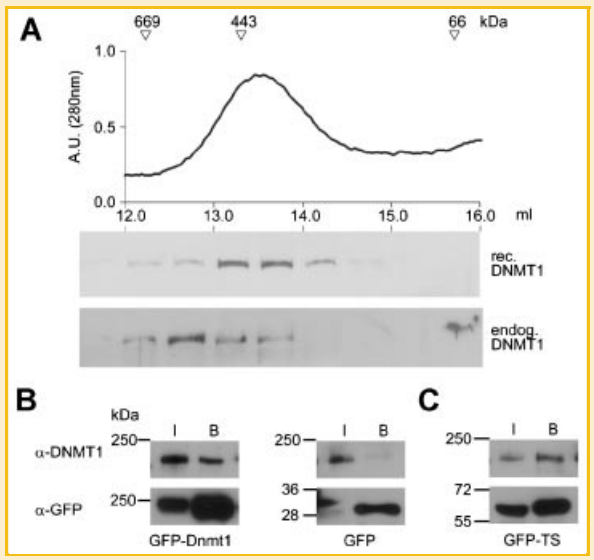

Fig. 1. DNMT1 was analyzed by gelfiltration and co-immunoprecipitation. A: Elution profile of recombinant human DNMT1 showing a peak at ~400 kDa, the *x*-axis indicates the protein fractions collected in 1 ml steps and the *y*-axis presents the absorption units (AU) at the wavelength of 280 nm. The arrows denote the molecular size of marker proteins applied in a separate run (thyroglobulin: 669 kDa, apoferritin 443 kDa, BSA 66 kDa). Immunoblot of elution fractions confirms the elution profile of recombinant DNMT1 (upper row). Endogenous DNMT1 of a HeLa cell extract is present in a higher molecular weight complex (lower row). B: Immunoblots after co-immunoprecipitations illustrate the interaction between GFP-Dnmt1 and endogenous DNMT1, whereas GFP alone was used as negative control. One percent of input and 30% of bound fractions were subjected to immunoblot analysis. The molecular size of the proteins (kDa) and the antibodies used are indicated. C Mapping the Dnmt1 dimerization to the TS domain of Dnmt1: Immunoblot after co-immunoprecipitation showing that the N-terminal TS domain of Dnmt1 can co-precipitate endogenous DNMT1.

MBP-TS fusion protein was eluted with 30 ml elution buffer (buffer CV + 10 mM Maltose). The peak fractions were combined and the TS domain was cleaved off the MBP moiety by incubation with TEV protease (Invitrogen) at 16°C over night. TEV protease and MBP were removed by a Q FF 5 ml column (GE Healthcare) and the TS domain was eluted with a step gradient.

RESULTS

Dnmt1 FORMS STABLE DIMERS

For biochemical characterization we purified (full-length) DNMT1 using a baculovirus expression system. Purified DNMT1 was loaded on a gelfiltration column and the elution profile was recorded (Fig. 1A). Immunoblot analysis of collected fractions showed that DNMT1 was eluted in a fraction corresponding to a molecular mass of about 400 kDa. This is approximately twofold the molecular mass of DNMT1 (183 kDa) indicating the presence of a dimeric DNMT1 complex. To analyze DNMT1 complex formation in vivo, we analyzed extracts from HeLa cells by gelfiltration and also did not observe a DNMT1 monomer fraction. Instead, the endogenous DNMT1 eluted as part of a higher molecular weight complex of 400–700 kDa which is likely caused by additional protein interactions occurring in living cells. The dimeric complex was stable under high salt buffer conditions up to 1 M NaCl. Dimer formation was further tested by co-immunoprecipitation experiments. GFP-Dnmt1 was expressed in transiently transfected HEK 293T cells and immunoprecipitated using the GFP-Nanotrap [Rothbauer et al., 2008]. Immunoblot analysis of input and bound fractions showed that the endogenous DNMT1 counterpart was efficiently co-precipitated (Fig. 1B).

THE N-TERMINAL TS DOMAIN MEDIATES Dnmt1 DIMERIZATION

The gelfiltration and co-immunoprecipitation experiments both indicated that DNMT1 forms a stable dimeric complex. To test whether this dimerization is related to the previously reported interaction between the N- and C-terminal domain [Fatemi et al., 2001; Margot et al., 2003] and to map the domains involved in this dimerization, we fused various parts of Dnmt1 with GFP and Cherry (Fig. 2A) and performed co-immunoprecipitation studies. We found that the TS domain was sufficient to precipitate the endogenous DNMT1 (Fig. 1C). To identify the part of Dnmt1 the TS domain binds to we co-expressed different GFP-Dnmt1 subdomains with Cherry-TS ($C_{310-629}$) in HEK 293T cells and performed co-immunoprecipitation. Input and bound fractions were analyzed by immunoblots against GFP and Cherry (Fig. 2A). GFP-N-terminus (G_{1-1111}) but not GFP-C-terminus ($G_{1124-1620}$) efficiently precipitated the TS domain $C_{310-629}$ pointing to a dimerization through the N-termini of two Dnmt1 molecules rather than an intermolecular interaction between the N- and C-terminal domain (Fig. 2B). Further fine-mapping showed that the TS domain $C_{310-629}$ efficiently co-precipitated with GFP-TS $G_{310-629}$ but not with G_{1-309} or $G_{630-1111}$ (Fig. 2b). These results show that Dnmt1 dimerization is mediated through a homotypic interaction of the N-terminal TS domain.

To independently verify these biochemical data in vivo, we performed a fluorescent two-hybrid assay (F2H), that allows direct visualization of protein interactions in single living cells [Zolghadr et al., 2008]. The F2H assay visualizes the interaction of a red fluorescent bait with a green fluorescent prey protein as co-localization at a defined nuclear spot. To anchor the fluorescent bait, we used a transgenic cell-line that contains a chromosomally integrated *lac* operator array and provides a defined binding platform for Lac repressor fusion proteins. We engineered a triple fusion protein comprising the TS domain as bait, the Lac repressor and the red fluorescent protein (RFP). Binding of the fusion protein (TS-LacI-RFP) to the *lac* operator array can directly be visualized as defined nuclear spot in living cells by fluorescence microscopy (Fig. 2C). Interaction of green fluorescent prey proteins with the TS domain leads to a co-localization at the anchor point (Fig. 2C, right panel) that is visible in the overlay as orange/yellow spot. With this assay we tested different Dnmt1 domains for interaction with the TS domain containing bait construct. We observed a clear co-localization of the N-terminal domain (G_{1-1111}) with the TS-LacI-RFP bait protein while the C-terminal domain ($G_{1124-1620}$) did not co-localize (Fig. 2C). To fine-map the interaction with the TS domain three parts of the N-terminal domain were tested and only $G_{310-629}$ showed co-localization with TS-LacI-RFP while the first and the last part (G_{1-309} or $G_{630-1111}$) did not interact and showed a diffuse distribution. These results show that the red labeled

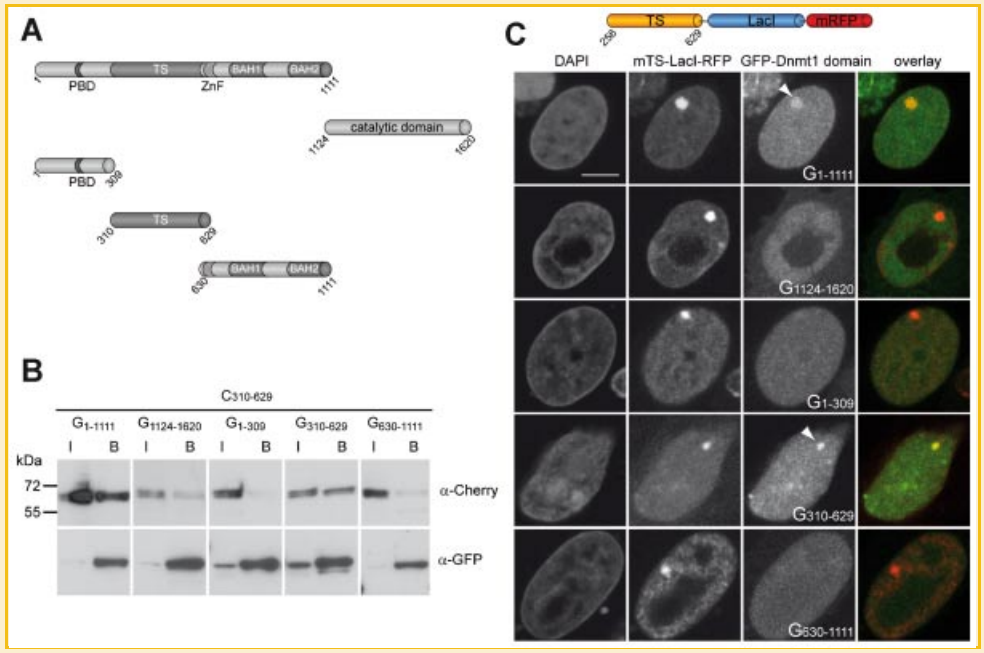

Fig. 2. N-terminal TS domain is the Dnmt1 dimerization domain. A: Schematic overview of Dnmt1 constructs used for co-immunoprecipitations. Subdomains are indicated: PBD, PCNA binding domain; TS, targeting sequence; ZnF, zinc finger; BAH1 + 2, bromo adjacent homology domains 1 + 2. B: Immunoblots after co-immunoprecipitations of GFP-Dnmt1 domains and Cherry-TS (C310–629) with the GFP-Nanotrap. G indicates GFP and C Cherry, numerics in subscript denote the first and last amino acids of Dnmt1 present in these constructs. One percent of input (I) and 20% of bound (B) fractions were subjected to SDS–PAGE, blotted on PVDF membrane (Millipore) and decorated with antibodies against Cherry and GFP. These results are representative of three independent experiments and show that GFP-N-terminus (G_{1-1111}) and GFP-TS ($G_{310-629}$) interact with Cherry-TS ($C_{310-629}$). C: Fluorescent two-hybrid (F2H) assay confirms biochemical interaction data. TS-LacI-RFP (bait, depicted on top) was co-expressed with GFP-Dnmt1 domains (prey) in transgenic BHK cells [Tsukamoto et al., 2000] containing a lac operator array. Binding of the TS-LacI-RFP fusion protein is visible as distinct nuclear spot and interaction of a GFP fusion protein leads to co-localizing fluorescence signals. DAPI, RFP, and GFP were imaged and an overlay image of GFP and RFP fluorescence is presented. The Dnmt1 Nterminus (G_{1-1111}) co-localizes with TS-LacI-RFP but the C-terminus ($G_{1124-1620}$) does not. From the three parts of the N-terminal domain only the TS domain ($G_{310-629}$) co-localized with TS-LacIRFP indicating a specific TS–TS interaction in vivo. The scale bar represents 5 μm.

TS domain interacts with green labeled TS domain in vivo. In summary, biochemical and cellular assays indicate that Dnmt1 dimerization is mediated by a direct intermolecular TS–TS domain interaction.

Dnmt1 DIMERIZATION IS FORMED BY A RATHER HYDROPHOBIC TS–TS INTERACTION

To test the complex formation properties we purified the TS domain that has a calculated molecular weight of about 30 kDa and analyzed it by gelfiltration. Immunoblot analysis of elution fractions showed a distinct peak at about 66 kDa corresponding to a TS dimer and high molecular weight complexes in the size range above 500 kDa indicating multimerization of the TS domain (Fig. 3A, lane 2). This supports the conclusion that the TS domain by itself can form a stable dimer and thus drive dimerization of DNMT1.

To analyze the nature and strength of this interaction, we performed co-immunoprecipitions of GFP-TS and Cherry-TS in the presence of increasing salt concentrations. We found that the interaction was stable despite the high ionic strength of the buffer containing 1 M NaCl (Fig. 3B) arguing for a more hydrophobic interaction. Indeed, the hydrophilicity plot [Hopp and Woods, 1981] of Dnmt1 shows that the TS domain is among the most hydrophobic parts of the regulatory domain of Dnmt1 (Fig. 3C). Taken together, these results indicate that the dimerization of Dnmt1 is mediated by a stable and rather hydrophobic interaction of the N-terminal TS domain.

Dnmt1 DIMERIZATION IS MEDIATED BY A BIPARTITE INTERFACE

To fine-map the dimerization interface we generated a series of GFP-TS deletion constructs including N- and C-terminal deletions in steps of about 50 amino acids. HEK 293T cells were co-transfected with GFP-TS deletion constructs and Cherry-TS ($C_{310-629}$) and co-precipitation experiments were performed. Surprisingly, all tested GFP-TS deletion proteins interacted with the Cherry-TS full-length domain (Supplementary Fig. 1) indicating a more complex and potentially multipartite interaction interface.

To further investigate the interacting regions of the domain, we generated additional GFP- and Cherry fusion proteins and tested interactions by co-immunoprecipitations (Fig. 4A). Pairs of TS subdomain constructs tested are depicted on the left side and their relative co-immunoprecipitation efficiency is shown in the bar graph on the right side. One representative immunoblot is displayed in Figure 4B. We observed no interaction between the N- and C-terminal parts of the TS domain (lane 3) arguing against a head-to-tail interaction. Interestingly, N- and C-terminal parts of the TS domain overlapping by 27 amino acids showed a strong interaction

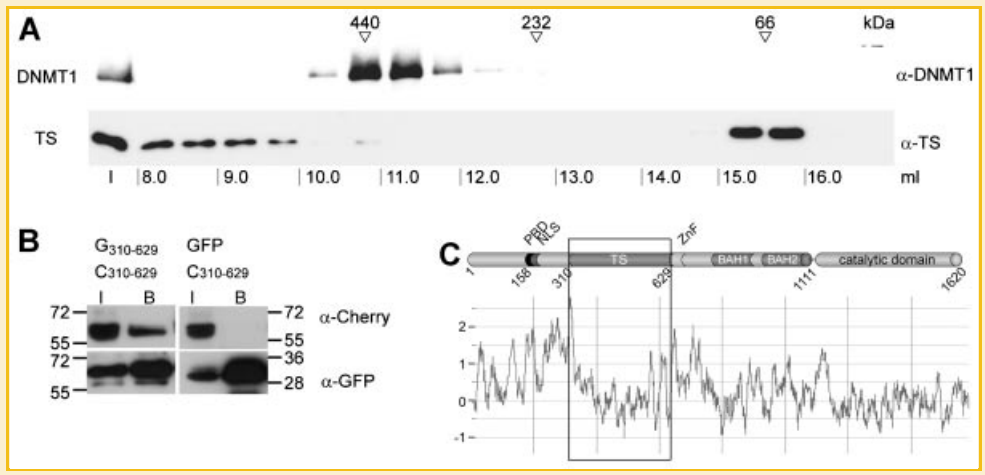

Fig. 3. Dnmt1 dimerization is formed by a rather hydrophobic TS–TS interaction. A: DNMT1 and the TS domain were studied by gelfiltration and the respective protein fractions are analyzed by immunoblots. The proteins and the migration of the size standards are indicated (in kDa) as well as the protein fractions loaded in ml and the input fraction (I). B: Hydrophilic or hydrophobic nature of the dimerization interaction was tested by co-immunoprecipitation of GFP-TS ($G_{310-629}$) and Cherry-TS ($G_{310-629}$) in buffer containing 1 M NaCl with subsequent immunoblot analysis. One percent of input (I) and 20% of bound (B) fractions were loaded and immunoblots probed with antibodies against GFP and Cherry. C (Top): Schematic outline of Dnmt1 full-length protein including subdomains: PBD (PCNA binding domain), NLS (nuclear localization signal). TS (targeting sequence), ZnF (zinc finger), BAH 1 + 2 (bromo adjacent homology domains 1 + 2). Bottom: Hydrophilicity plot [Hopp and Woods, 1981] of the Dnmt1 protein sequence generated with the ProtScale tool of the ExPASy proteomics server (http://www.expasy.ch/tools/protscale.html) with the linear weight variation model and a 15 amino acid window. Hydrophobic regions are represented as minima in the plot; a rectangle marks the TS domain which is rather hydrophobic in comparison with the rest of the N-terminus.

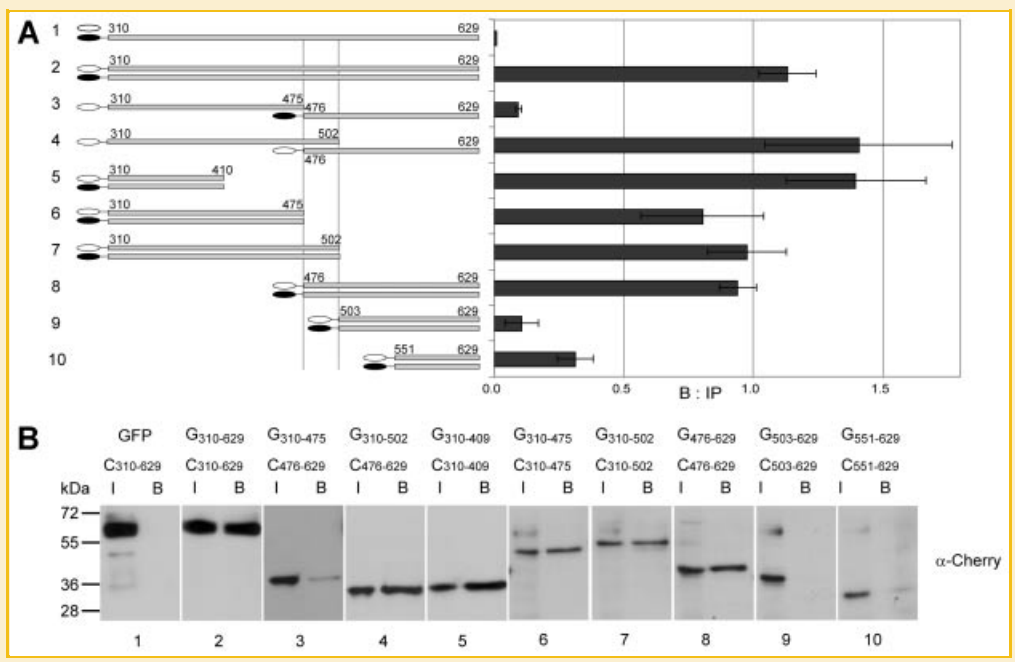

Fig. 4. Fine-Mapping of the TS–TS interactions by co-immunoprecipitation analyses. A (Left panel): Scheme of GFP (open ellipse) and Cherry (filled ellipse) tagged TS deletion constructs used for immunoprecipitation assays: Numbers above the construct refer to respective amino acid positions within Dnmt1. Right panel: Bar graph shows relative co-immunoprecipitation rates. Western blot signals from input and bound fractions were quantified with ImageJ and mean ratios of three independent experiments ± standard error (SE) determined. B: Immunoblot from one representative co-immunoprecipitation experiment out of three independent experiments. Quantification of all three experiments is shown above in (A). G indicates GFP, C indicates Cherry. One percent of input (I) and 20% of bound (B) fractions were subjected to SDS–PAGE and immunoblotting and probed with antibodies against Cherry. Precipitation efficiency of GFP-proteins was checked by immunoblot analysis with antibodies against GFP (not shown). Molecular marker sizes are indicated on the left.

(lane 4) indicating that this middle part plays an important role in the TS–TS interaction. In addition, we found that the N-terminal part but not the C-terminal part of the TS domain can dimerize. These results indicate that dimerization is mediated by a bipartite interface containing the N-terminal (aa 310–409) and the central part (aa 476–502) of the TS domain. It should be noted that the hydrophobic nature of the TS domain makes the fine-mapping of the dimerization interface difficult and may lead to false-positive results. Further alanine scanning mutagenesis [Fellinger et al., 2008] of the TS domain did not yield specific dimerization mutants (data not shown) which is probably due to the large bipartite interaction surface spanning almost 200 amino acids.

Larger deletions within the TS domain were previously shown to abolish catalytic activity of Dnmt1 [Fig. 5A, Margot et al., 2000; Zimmermann et al., 1997] emphasizing the importance of the TS domain. However, it is unclear to what extent this is due to disruption of dimerization, since the TS domain also mediates association with heterochromatin [Easwaran et al., 2004] and may also contribute to the allosteric activation of the catalytic domain [Margot et al., 2000; Fatemi et al., 2001].

Interestingly, sequence alignments of Dnmt1 homologs showed that the core region of the TS domain that is involved in dimerization is highly conserved from human to plants (Fig. 5A). The crystal structure shows that the conserved core region consists of three β-sheets forming part of a potential binding pocket in the TS domain (Fig. 5B). The high conservation and distinct structure of this TS core region suggests an essential role in Dnmt1 regulation.

DISCUSSION

Recent work has shown that DNA methylation is linked with several other nuclear processes and involves numerous protein interactions. Analyzing recombinant and endogenous Dnmt1 protein fractions we found that Dnmt1 forms a stable dimer. We mapped the dimerization domain to the N-terminal TS domain of Dnmt1 using

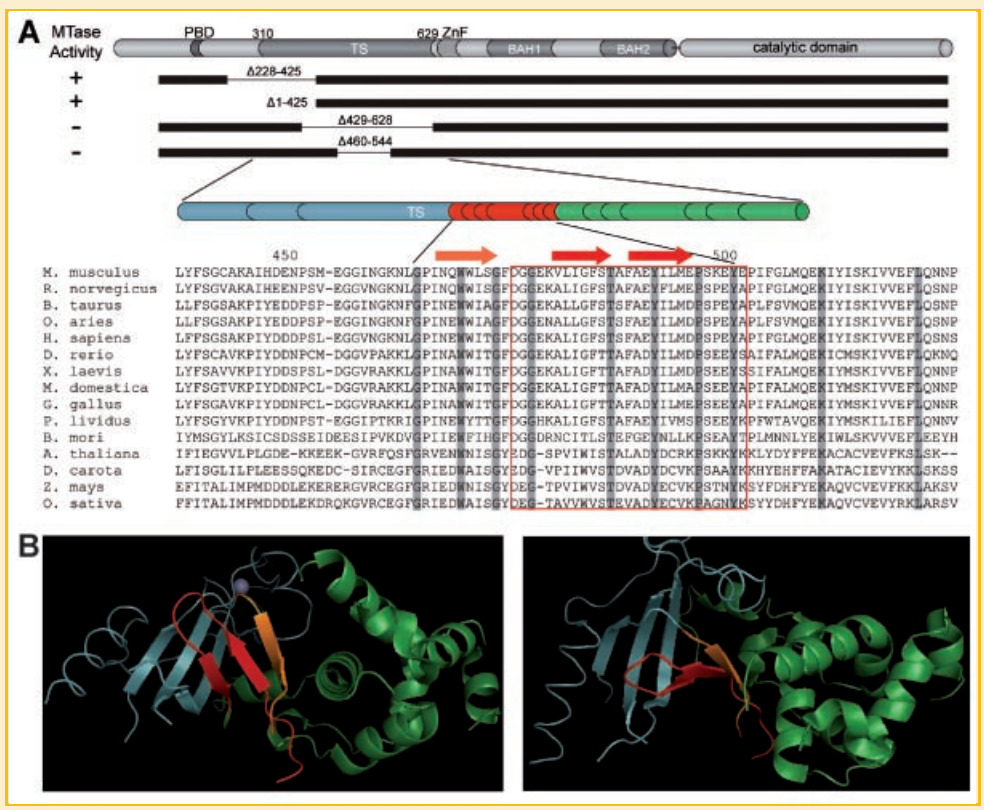

Fig. 5. TS domain is crucial for Dnmt1 activity and contains a highly conserved core region. A: Schematic overview of Dnmt1 and subdomains (PBD, PCNA binding domain; TS, targeting sequence; ZnF, zinc finger; BAH1 + 2, bromo adjacent homology domains1 + 2). Below, Dnmt1 deletion mutants and their in vitro activity (left) are shown, results were taken from Margot et al. [2000]. Below, a magnified overview of the TS domain is depicted with an N-terminal part (blue), the highly conserved core (red) and the C-terminal part (green). Black lines represent amino acids that are identical in Dnmt1 homologs from human to plants. Below, a ClustalW alignment of the central TS region from selected Dnmt1 homologs is shown. Identical amino acids are marked by dark gray shading. Red rectangle highlights the 27 amino acids which are important for TS–TS dimerization. Accession numbers: M. musculus, P13864; R. norwegicus, Q9Z330; B. taurus, Q24K09; O. aries, Q865V5; H. sapiens, P26358; D. rerio, Q8QGB8; X. laevis, Q6GQH0; M. domestica, Q8MJ28; G. gallus, Q92072; P. lividus, Q27746; B. mori, Q5W7N6; A. thaliana, Q9SEG3; D. carota, O48867; Z. mays, Q8LPU6; O. sativa, A2XMY1. B: Crystal structure of human TS domain (aa 351–600; Protein Data Bank 3epz). The image was generated using PyMOL [DeLano 2002]. The N-terminal part of the TS domain is colored in blue and coordinates a zinc-ion, the highly conserved central region in orange and red and the C-terminal region in green. The view from two angles shows the highly conserved β-sheet structure (orange/red) of the TS domain as part of a potential binding pocket.

gelfiltration, co-immunoprecipitation and in vivo fluorescent two-hybrid assay. Fine-mapping identified a homotypic TS–TS interaction containing a bipartite dimerization interface spanning about 200 amino acids of the TS domain.

Interestingly, dimerization has also been shown for other C5 DNA methyltransferases including the bacteria HhaI and the vertebrate Dnmt3a and Dnmt3L [Dong et al., 2004; Jia et al., 2007]. The crystal structure revealed that the central Dnmt3a dimer is flanked by Dnmt3L forming a 3L-3a-3a-3L tetramer. Disruption of the Dnmt3a dimer by specific point mutations resulted in loss of catalytic activity [Jia et al., 2007]. In contrast to these DNA methyltransferases that dimerize via the catalytic domain, Dnmt1 dimerization is mediated by its unique regulatory, N-terminal domain. Consistent with this difference, the key residues for Dnmt3a dimerization (R881 and D872) are not conserved in Dnmt1. In addition to dimerization, the TS domain of Dnmt1 also seems to contribute to allosteric activation of the catalytic domain [Zimmermann et al., 1997; Margot et al., 2000; Fatemi et al., 2001] and mediates association with heterochromatin [Easwaran et al., 2004]. Further studies are necessary to elucidate the temporal and spatial coordination of these multiple functions of the TS domain.

ACKNOWLEDGMENTS

We thank Bijàn Montazeri for practical support, Kourosh Zolghadr for introduction to the F2H assay, Andrea Rottach and Fabio Spada for discussion and critical reading of the manuscript. We thank R.Y. Tsien for mCherry DNA and D. Spector for the transgenic BHK cell line. This work has been supported by grants from the Deutsche Forschungsgemeinschaft to HL and GL and the Nanosystems Initiative Munich (NIM). KF is a fellow of the International Max Planck Research School (IMPRS) for Molecular and Cellular Life Sciences.

REFERENCES

Bestor TH, Ingram VM. 1983. Two DNA methyltransferases from murine erythroleukemia cells: Purification, sequence specificity, and mode of interaction with DNA. Proc Natl Acad Sci USA 80:5559–5563.

Bird A. 2002. DNA methylation patterns and epigenetic memory. Genes Dev 16:6–21.

Bostick M, Kim JK, Esteve PO, Clark A, Pradhan S, Jacobsen SE. 2007. UHRF1 plays a role in maintaining DNA methylation in mammalian cells. Science 317:1760–1764.

Chuang LS, Ian HI, Koh TW, Ng HH, Xu G, Li BF. 1997. Human DNA-(cytosine-5) methyltransferase-PCNA complex as a target for p21WAF1. Science 277:1996–2000.

DeLano WL. 2002. The PyMOL molecular graphics system. Palo Alto, CA, USA: DeLano Scientific.

Dong A, Zhou L, Zhang X, Stickel S, Roberts RJ, Cheng X. 2004. Structure of the Q237W mutant of HhaI DNA methyltransferase: An insight into protein-protein interactions. Biol Chem 385:373–379.

Easwaran HP, Schermelleh L, Leonhardt H, Cardoso MC. 2004. Replication-independent chromatin loading of Dnmt1 during G2 and M phases. EMBO Rep 5:1181–1186.

Egger G, Jeong S, Escobar SG, Cortez CC, Li TW, Saito Y, Yoo CB, Jones PA, Liang G. 2006. Identification of DNMT1 (DNA methyltransferase 1) hypomorphs in somatic knockouts suggests an essential role for DNMT1 in cell survival. Proc Natl Acad Sci USA 103:14080–14085.

Esteve PO, Chin HG, Smallwood A, Feehery GR, Gangisetty O, Karpf AR, Carey MF, Pradhan S. 2006. Direct interaction between DNMT1 and G9a coordinates DNA and histone methylation during replication. Genes Dev 20:3089–3103.

Fatemi M, Hermann A, Pradhan S, Jeltsch A. 2001. The activity of the murine DNA methyltransferase Dnmt1 is controlled by interaction of the catalytic domain with the N-terminal part of the enzyme leading to an allosteric activation of the enzyme after binding to methylated DNA. J Mol Biol 309: 1189–1199.

Fellinger K, Leonhardt H, Spada F. 2008. A mutagenesis strategy combining systematic alanine scanning with larger mutations to study protein interactions. Anal Biochem 373:176–178.

Gaudet F, Hodgson JG, Eden A, Jackson-Grusby L, Dausman J, Gray JW, Leonhardt H, Jaenisch R. 2003. Induction of tumors in mice by genomic hypomethylation. Science 300:489–492.

Gaudet F, Rideout WM III, Meissner A, Dausman J, Leonhardt H, Jaenisch R. 2004. Dnmt1 expression in pre- and postimplantation embryogenesis and the maintenance of IAP silencing. Mol Cell Biol 24:1640–1648.

Goll MG, Bestor TH. 2005. Eukaryotic cytosine methyltransferases. Annu Rev Biochem 74:481–514.

Hermann A, Gowher H, Jeltsch A. 2004. Biochemistry and biology of mammalian DNA methyltransferases. Cell Mol Life Sci 61:2571–2587.

Hopp TP, Woods KR. 1981. Prediction of protein antigenic determinants from amino acid sequences. Proc Natl Acad Sci USA 78:3824–3828.

Jia D, Jurkowska RZ, Zhang X, Jeltsch A, Cheng X. 2007. Structure of Dnmt3a bound to Dnmt3L suggests a model for de novo DNA methylation. Nature 449:248–251.

Leonhardt H, Cardoso MC. 2000. DNA methylation, nuclear structure, gene expression and cancer. J Cell Biochem Suppl 35:78–83.

Leonhardt H, Page AW, Weier HU, Bestor TH. 1992. A targeting sequence directs DNA methyltransferase to sites of DNA replication in mammalian nuclei. Cell 71:865–873.

Li E, Bestor TH, Jaenisch R. 1992. Targeted mutation of the DNA methyltransferase gene results in embryonic lethality. Cell 69:915–926.

Margot JB, Aguirre-Arteta AM, Di Giacco BV, Pradhan S, Roberts RJ, Cardoso MC, Leonhardt H. 2000. Structure and function of the mouse DNA methyltransferase gene: Dnmt1 shows a tripartite structure. J Mol Biol 297:293–300.

Margot JB, Ehrenhofer-Murray AE, Leonhardt H. 2003. Interactions within the mammalian DNA methyltransferase family. BMC Mol Biol 4:7.

Mortusewicz O, Schermelleh L, Walter J, Cardoso MC, Leonhardt H. 2005. Recruitment of DNA methyltransferase I to DNA repair sites. Proc Natl Acad Sci USA 102:8905–8909.

Myant K, Stancheva I. 2008. LSH cooperates with DNA methyltransferases to repress transcription. Mol Cell Biol 28:215–226.

Pradhan S, Bacolla A, Wells RD, Roberts RJ. 1999. Recombinant human DNA (cytosine-5) methyltransferase. I. Expression, purification, and comparison of de novo and maintenance methylation. J Biol Chem 274:33002–33010.

Rothbauer U, Zolghadr K, Muyldermans S, Schepers A, Cardoso MC, Leonhardt H. 2008. A versatile nanotrap for biochemical and functional studies with fluorescent fusion proteins. Mol Cell Proteomics 7:282–289.

Rottach A, Kremmer E, Nowak D, Leonhardt H, Cardoso MC. 2008. Generation and characterization of a rat monoclonal antibody specific for multiple red fluorescent proteins. Hybridoma (Larchmt) 27:337–343.

Schermelleh L, Haemmer A, Spada F, Rosing N, Meilinger D, Rothbauer U, Cardoso MC, Leonhardt H. 2007. Dynamics of Dnmt1 interaction with the replication machinery and its role in postreplicative maintenance;1; of DNA methylation. Nucleic Acids Res 35:4301–4312.

Shaner NC, Campbell RE, Steinbach PA, Giepmans BN, Palmer AE, Tsien RY. 2004. Improved monomeric red, orange and yellow fluorescent proteins derived from Discosoma sp. red fluorescent protein. Nat Biotechnol 22:1567–1572.

Sharif J, Muto M, Takebayashi S, Suetake I, Iwamatsu A, Endo TA, Shinga J, Mizutani-Koseki Y, Toyoda T, Okamura K, Tajima S, Mitsuya K, Okano M, Koseki H. 2007. The SRA protein Np95 mediates epigenetic inheritance by recruiting Dnmt1 to methylated DNA. Nature 450:908–912.

Spada F, Haemmer A, Kuch D, Rothbauer U, Schermelleh L, Kremmer E, Carell T, Langst G, Leonhardt H. 2007. DNMT1 but not its interaction with the replication machinery is required for maintenance of DNA methylation in human cells. J. Cell Biol 176:565–571. 10.1083/jcb.200610062.

Tsukamoto T, Hashiguchi N, Janicki SM, Tumbar T, Belmont AS, Spector DL. 2000. Visualization of gene activity in living cells. Nat Cell Biol 2:871–878.

Vire E, Brenner C, Deplus R, Blanchon L, Fraga M, Didelot C, Morey L, Van Eynde A, Bernard D, Vanderwinden JM, Bollen M, Esteller M, Di Croce L, de Launoit Y, Fuks F. 2006. The Polycomb group protein EZH2 directly controls DNA methylation. Nature 439:871–874.

Yokochi T, Robertson KD. 2002. Preferential methylation of unmethylated DNA by Mammalian de novo DNA methyltransferase Dnmt3a. J Biol Chem 277:11735–11745.

Zimmermann C, Guhl E, Graessmann A. 1997. Mouse DNA methyltransferase (MTase) deletion mutants that retain the catalytic domain display neither de novo nor maintenance methylation activity in vivo. Biol Chem 378:393–405.

Zolghadr K, Mortusewicz O, Rothbauer U, Kleinhans R, Goehler H, Wanker EE, Cardoso MC, Leonhardt H. 2008. A fluorescent two-hybrid assay for direct visualization of protein interactions in living cells. Mol Cell Proteomics 7:2279–2287.